Journal of Pharmaceutical and Biomedical Analysis 248 (2024) 116267

Contents lists available at ScienceDirect

Journal of Pharmaceutical and Biomedical Analysis

journal homepage: www.journals.elsevier.com/journal-of-pharmaceutical-and-biomedical-analysis

Andrographolide targets EGFR to impede epithelial–mesenchymal transition in human breast cancer cells

Chutima Kaewpiboon [a,*], Nawong Boonnak [b], Abdul-Wahab Salae [c], Sirichatnach Pakdeepromma [d], Natpaphan Yawut [e,f], Young-Hwa Chung [g,*]

[a] Department of Biology, Faculty of Science and Digital Innovation, Thaksin University, Phatthalung 93210, Thailand
[b] Department of Basic Science and Mathematics, Faculty of Science and Digital Innovation, Thaksin University, Songkhla 90000, Thailand
[c] Department of Science and Mathematics, Faculty of Science and Technology, Phuket Rajabhat University, Phuket 83000, Thailand
[d] Department of General Science and Liberal Arts, King Mongkut's Institute of Technology Ladkrabang Prince of Chumphon Campus, Pathiu, Chumphon 86160, Thailand
[e] Office of Research Administration, Chiang Mai University, Chiang Mai 50200, Thailand
[f] Department of Industrial Engineering, Faculty of Engineering, Chiang Mai University, Chiang Mai 50200, Thailand
[g] Department of Cogno-Mechatronics Engineering, Pusan National University, BK 21+, Busan 46241, Republic of Korea

ARTICLE INFO

Keywords:
Breast cancer cells
Andrographolide
Epithelial-mesenchymal transition
EGFR

ABSTRACT

Despite the primary surgical treatment for breast cancer patients, malignant invasiveness and metastasis remain threatening factors for women with breast cancer. As chemotherapy yields unsatisfactory results, it prompted us to search for effective natural agents with few side-effects. Although andrographolide (ADGL), a natural diterpenoid lactone isolated from *Andrographis paniculata*, presents anticancer effects, the molecular mechanism remains unknown. Initially, on comparing the expression of proteins related to epithelial–mesenchymal transition (EMT) between nonmetastatic cancer MCF7 cells and highly metastatic cancer MDA-MB-231 cells, we found that MDA-MB-231 cells exhibit higher protein levels of N-cadherin and vimentin and lower protein levels of E-cadherin when compared to MCF7 cells. Moreover, MDA-MB-231 cells also exhibited higher EGFR expression and activity, higher STAT1 activity and abundant HDAC4 expression. To elucidate whether these proteins are closely associated with EMT, EGFR, STAT1 or HDAC4, the proteins were silenced in MDA-MB-231 breast cancer cells by their specific siRNAs. We found that silencing these proteins reduced EMT, indicating an important role of EGFR, STAT1 and HDAC4 in EMT progression. When we treated MDA-MB-231 cells with ADGL as a potential therapeutic drug, we found that ADGL treatment inhibited cell migration and invasion. Furthermore, it also recovered E-cadherin expression and decreased N-cadherin and vimentin protein levels. ADGL treatment reduced EGFR expression at a lower concentration (1 μg/mL); however, STAT1 activity and HDAC4 expression was reduced by a higher concentration (5 μg/mL) of ADGL. Moreover, we observed that the combined treatment with ADGL and siRNAs against these proteins highly sensitized the MDA-MB-231 cells to apoptosis compared to that with ADGL and control siRNA. Collectively, our results suggest that ADGL targets EGFR, thereby inhibiting EMT in human breast cancer cells.

1. Introduction

Recently, the World Health Organization reported that breast cancer is the most frequently diagnosed cancer in women worldwide, and comprises 16 % of all female cancers. Moreover, a major hurdle in breast cancer therapy is that breast cancer patient's present metastasis after initial response to the standard care therapy. Epithelial–mesenchymal transition (EMT) imparts metastatic potential to epithelial cancer cells, enabling them to invade, migrate and subsequently disseminate to form distant metastases resulting in a noncurable disease. EMT facilitates an increase in the subpopulation of cancer stem cells (CSCs) and is associated with a chemoresistant phenotype in breast cancer [1]. EMT is a multistep process involving the gradual loss of cell–cell adhesions and tight junctions leading to cytoskeleton reorganization and loss of apical polarity, which eventually enables a cancer cell of epithelial origin to attain spindeloid morphology. Pharmacological inhibition of EMT can potentially lead to reversion of aggressive breast cancer cells to a more differentiated epithelial phenotype by inducing mesenchymal–epithelial

* Corresponding authors.
E-mail addresses: chutima.k@tsu.ac.th (C. Kaewpiboon), younghc@pusan.ac.kr (Y.-H. Chung).

https://doi.org/10.1016/j.jpba.2024.116267
Received 13 January 2024; Received in revised form 18 May 2024; Accepted 28 May 2024
Available online 5 June 2024

transition (MET) in order to prevent metastasis and distant recurrence.

In recent years, bioactive components from plants used in traditional Asian medicine have been shown to be effective as potential cancer preventive as well as therapeutic agents. Leaves from *Andrographis paniculata* plant species have been successfully used in the traditional Thai medicine. *A. paniculata* is widely used to prevent common cough and colds, remove body heat, dispel toxins from the body and acts as an antidote against snake and insect poisons [2]. Moreover, the plant has been reported to exhibit various *in vivo* as well as *in vitro* biological activities such as antidiabetic [3], antiviral [4], anti-inflammatory [5], anti-HIV [6], immunomodulatory [7] and anticancer [8] activities. The medicinal benefits of *A. paniculata* have been attributed to a natural diterpenoid lactone, andrographolide (ADGL), isolated from the extract of *A. paniculata* leaves. The anticancer activities of ADGL, such as suppression of angiogenesis [9] and cell migration, invasion [10] and proliferation [11] have been reported in multiple cancer cell lines and tumor models. Cellular studies have provided novel insights into the mechanisms underlying the anticancer effects of ADGL. For example, ADGL inhibits the proliferation of human breast cancers via suppressing COX-2 expression at both protein and mRNA levels [9]. In MCF-7 breast cancer cells, andrographolide inhibited MMP-9 protein expression and its enzyme activity, and suppressed cell migration and invasion [12]. Moreover, ADGL reduced the levels of phosphorylated Akt (Ser473) and Akt (Thr308) in the treated cells [13] and inhibited matrix metalloprotein (MMP)-mediated cell proliferation and migration in T47D and MDA-MB-231 cells [14]. Moreover, EGFR is upregulated in various cancers involving the lung [15], gliomas [16], ovaries [17] and breast [18]. As a result, EGFR is considered a prime target in the development of cancer therapies [19], and hence, is emphasized in our present study. Interestingly, we found that ADGL targets EGFR, thereby inhibiting EMT at an early stage in cancer metastasis. Therefore, the study investigated the potential of andrographolide, isolated from *A. paniculata*, in inhibiting EMT in breast cancer cells and elucidated the underlying molecular mechanisms.

2. Materials and methods

2.1. Materials and reagents

All the chemicals, reagents and solvents used in the study were of reagent grade. The cell lines namely, Human breast cancer; MCF-7 (low invasive, estrogen-responsive cells) and MDA-MB-231 (high invasive, estrogen nonresponsive) cell lines were purchased from ATCC, Manassas, VA, USA. Dulbecco's modified Eagle medium (DMEM) fetal bovine serum (FBS) penicillin, and streptomycin (PEN/STEP) were purchased from Gibco (Grand Island, NY, USA). The reagents namely, NaCl (sodium chloride), NP-40 (nonylphenoxypolyethoxyethanol), Tris-HCl [tris (hydroxymethyl)-aminomethane-hydrochloric acid, Na_2VO_3 (sodium orthovanadate), NaF (sodium fluoride) and protease inhibitors were purchased from Sigma-Aldrich and Merck Life Science Private Limited (Bangkok, Thailand). The primary antibodies for western blotting assay namely, cleaved poly (ADP-ribose) polymerase (PARP; Asp214) and HDAC4 antibodies were purchased from Cell Signaling Biotechnology (Beverly, MA, USA), Actin (C4), STAT1, and p-STAT1 antibodies were purchased from Santa Cruz Biotechnology (Santa Cruz, CA, USA), EGFR, p-EGFR, E-cadherin, N-cadherin and vimentin antibodies and the secondary antibodies for western blotting assay namely, horseradish peroxidase-conjugated with rabbit or mouse immunoglobulin G were purchased from Abcam (Cambridge, MA, USA). The secondary antibody for immunofluorescence assay namely; Alexa Fluor 418-conjugated goat anti-mouse and donkey anti-rabbit antibody were purchased from Molecular Probes (Eugene, OR, USA). The reagents for short interference **(Si)** RNA transfection namely; Sicontrol, SiEGFR, SiHDAC4 and SiSTAT1 were purchased from Bioneer (Daejeon, Korea). Lipofectamine 2000 was purchased from Invitrogen (Carlsbad, CA, USA). The reagent for Transwell invasion assay namely; Matrigel was purchased from BD Biosciences (FL, USA).

2.2. Collection of plant material

Leaves of *A. paniculata* were collected in August 2018 from Songkhla Province, southern part of Thailand. Botanical identification was done by Ubonwan Upho, Ph.D. and Miss Manee Keawchanid from Thaksin University. A voucher specimen (No. 1(A)1) has been deposited at the Thaksin University Plant Herbarium.

2.3. Isolation and characterization of andrographolide

Ground-dried leaves of *A. paniculata* (500 g) were extracted with $CHCl_3$ (for 72 h) at room temperature and were further evaporated under reduced pressure to afford a greenish crude $CHCl_3$ extract, which was defatted with *n*-hexane and then subjected to quick column chromatography (QCC) eluting with increasing polarities of 0–70 % v/v of EtOAc in *n*-hexane to yield 10 fractions (F1-F10). Fraction F4 was further separated by column chromatography (CC) with a gradient of 0–70 % v/v of EtOAc in *n*-hexane to afford 5 subfractions (F4A-F4E) and ADGL (86.3 mg), which was recrystallized from the $CHCl_3$-CH_3OH (8:2 v/v) to give plate-shaped colorless single crystals of ADGL [20]. The structure of ADGL was analyzed by melting point, FT-IR, ^{1}H NMR (Supplementary Fig. 1s and Table 1s) and ^{13}C NMR (Supplementary Fig. 2 s). The purity of the compound has been evaluated with thin-layer chromatography (TLC) and High-performance liquid chromatography (HPLC) (Supplementary Fig. 3 s).

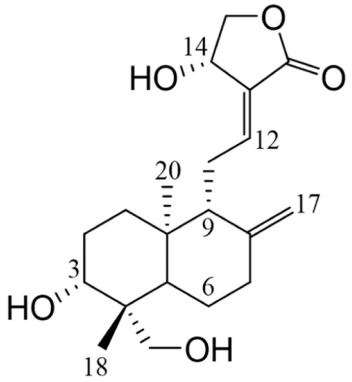

ADGL

2.4. Preparation of cell cultures

Human breast cancer; MCF-7 (low invasive, estrogen-responsive cells) and MDA-MB-231 (high invasive, estrogen nonresponsive) cell lines were cultured in Dulbecco's modified Eagle medium (DMEM), supplemented with 10 % fetal bovine serum (FBS), 1 % penicillin, and streptomycin at 37 °C in a humidified atmosphere of 5 % carbon dioxide (CO_2) in air.

2.5. Western blotting assay

MCF-7 and MDA-MB-231cell lines were harvested and lysed with the lysis buffer (150 mM NaCl, 1 % NP-40, 50 mM Tris-HCl pH 7.5 containing 0.1 mM Na_2VO_3, 1 mM NaF and protease inhibitors. For immunoblotting, proteins from the whole-cell lysates were resolved by 10 % or 12 % sodium dodecyl sulfate (SDS)-polyacrylamide gel electrophoresis (PAGE) and then transferred to nitrocellulose membranes. Primary antibodies namely, cleaved poly (ADP-ribose) polymerase (PARP; Asp214) and HDAC4 antibodies. Actin (C4), STAT1 and p-STAT1

antibodies were used at 1:1000 or EGFR, p-EGFR, E-cadherin, N-cadherin and vimentin antibodies were used at 1:2000 dilutions and secondary antibodies, horseradish peroxidase-conjugated with rabbit or mouse immunoglobulin G was used at 1:2000 dilutions in 5 % nonfat dry milk. After the final washing step, the nitrocellulose membranes were subjected to an enhanced chemiluminescence assay using the LAS 4000 mini. Densitometric analysis of protein expression levels from all experiments were performed using ImageJ software for density of protein band analysis. The visualization of β-actin was used to ensure equal sample loading in each lane. All experiments were repeated at least 3 times.

2.6. Immunofluorescence assay

MCF-7 and MDA-MB-231cell lines were fixed with 4 % paraformaldehyde for 15 min, permeabilized with cold acetone for 15 min, blocked with 10 % goat serum for 30 min, and treated with primary antibodies (1:100 dilutions) for 30 min at room temperature. After incubation, the cells were washed extensively with PBS, incubated with Alexa Fluor 418-conjugated goat anti-mouse or donkey anti-rabbit antibody (1:500 dilution) in PBS for 30 min at room temperature, and were then washed thrice with PBS. For nuclear staining, the cells were incubated with DAPI for 5 min in the dark and washed thrice with PBS. The stained cells were mounted using PBS containing 10 % glycerol and the images were observed using a fluorescence microscope. The MDA-MB-231cell lines was treated with ADGL (5.0 μg/mL) and then was examined phospho-EGFR protein expression levels using immunofluorescence assay.

2.7. Short interference RNA transfection

MDA-MB-231 cell line were trypsinized and incubated overnight to achieve 60 %–70 % confluency before small interfering RNA (SiRNA) transfection. Human STAT1-siRNAs (100 nM), human HDAC4-SiRNAs (100 nM), or negative control SiRNAs (100 nM) were mixed with Lipofectamine 2000. The cells were incubated with the transfection mixture for 24 h and were then rinsed with DMEM medium containing 10 % fetal bovine serum. The cells were incubated for 24 h before harvest. In the ADGL combination, the transfected cell was incubated in the medium with or without ADGL at 5 μg/mL for 24 h after transfection with a control SiRNA or SiRNAs against EGFR, STAT1 or HDAC4 before harvest for western blotting assay.

2.8. Wound-healing assay

MDA-MB-231 cell line or SiEGFR, SiHDAC4, SiSTAT1 and Sicontrol transfected cell line (1×10^5 cells/well) were plated in the growth medium in 24-well plates and incubated for 24 h. After confirming the formation of a complete monolayer. The monolayer was washed twice with PBS to remove debris or the detached cells from the monolayer, and then medium with or without ADGL by various concentrations (1, 5 and 10 ug/mL) was added the cells and incubated for 24 h. Migration and cell movement throughout the wound area were visualized and photographed under a phase-contrast microscope at 0, 12 and 24 h. The cell wound closure rate was calculated using the following equation: Wound closure = [1-(wound area at Tt/wound area at T0)] × 100, where Tt is the time passed since wounding and T0 is the time the wound was created. The experiments were performed in triplicate.

2.9. Transwell invasion assay

Cell invasive capacity of MDA-MB-231 cell line or SiEGFR, SiHDAC4, SiSTAT1 and Sicontrol transfected cell (5×10^4 cells per well) were determined using a Transwell Filter (8 μm pore size, Corning) with Matrigel. Briefly, PC cells treated with ADGL combination were transferred in each upper chamber in 200 μL of serum-free medium, and then 500 μL of complete medium was added into each bottom chamber with the same concentration of ADGL. After incubation for 24 h, the cells in the upper chamber were removed, and the invading cells in the membrane were stained with hematoxylin–eosin. The stained cells were photographed and counted under a light microscope in at least six randomly-selected fields.

2.10. Cell viability assay

The 3-(4,5-dimethylthiazol-2-yl)-2,5-diphenyltetrazolium bromide (MTT) assay was performed for the measurement of cell survival as previously described [21]. Dye solution containing tetrazolium was added to the cells in the 96-well plate and incubated for 2 h. The absorbance of the formazan produced by living cells was measured at 570 nm. The relative percentage of cell survival was calculated using the following equation: % cell survival = (OD_T / OD_C), where OD_T is the mean absorbance of the treated cell and OD_C is the mean absorbance of the control cell.

2.11. Statistical analysis

Data are presented as a means ± standard deviation (S.D.) with n=3. Statistical analyses were performed with the One-way Anova using GraphPad Instat (GraphPad software, San Diego, CA, USA). Values significantly different from the control are presented by $^*P < 0.05$, $^{**}P < 0.01$, and $^{***}P < 0.001$.

3. Results and discussion

3.1. MDA-MB-231 cells exhibit more drastic features of EMT compared to the MCF-7 cells

Epithelial to mesenchymal transition (EMT) progression is a crucial step that precedes the induction of motility and invasive potential during metastatic progression of malignant cells. Biochemical hallmarks of EMT reversal include gain of expression in the epithelial marker proteins such as E-cadherin with a concomitant decrease in the mesenchymal marker (e.g., vimentin and N-cadherin) expression [22]. Several studies have linked EMT to the invasive and metastatic potential of breast cancer cells [23]. A feature of EMT includes the suppression of E-cadherin expression, which disrupts the activation of signaling pathways that control cell migration, invasion and metastasis [24]. To investigate the correlation of metastatic properties and biochemical features, we compared the expression of protein related to EMT between a non-metastatic cancer cell line (MCF-7) and one highly metastatic cancer cell line (MDA-MB-231). We found that the protein levels of N-cadherin and vimentin were upregulated and E-cadherin expression was decreased in the MDA-MB-231 cells compared to those in the MCF-7 cells (Fig. 1A). Immunofluorescent microscopy confirmed the lower levels of E-cadherin in MDA-MB-231 cells and higher levels of E-cadherin in MCF-7 cells (Fig. 1B). As we observed that upregulation of EGFR, STAT1 and HDAC4 was involved in drug resistance as well as EMT in the cancer cells overexpressing cancer upregulated gene (CUG)2 [25], we explored the protein levels in both breast cancer cells. MDA-MB-231 cells exhibited higher levels of p-EGFR, EGFR, p-STAT1 and HDAC4 compared to those in MCF-7 cells (Fig. 1C). Moreover, enhanced levels of EGFR protein were detected in the MDA-MB-231 cells rather than MCF-7 cells (Fig. 1D). Based on this result, we thus assume that higher levels of p-EGFR, EGFR, p-STAT1 and HDAC4 might be involved in the metastatic properties of breast cancer cells as seen in the cancer cells overexpressing CUG2 [25].

3.2. Silencing EGFR, STAT1, or HDAC4 inhibits EMT in MDA-MB231 breast cancer cells

As we observed the elevated expression or activity of EGFR, STAT1

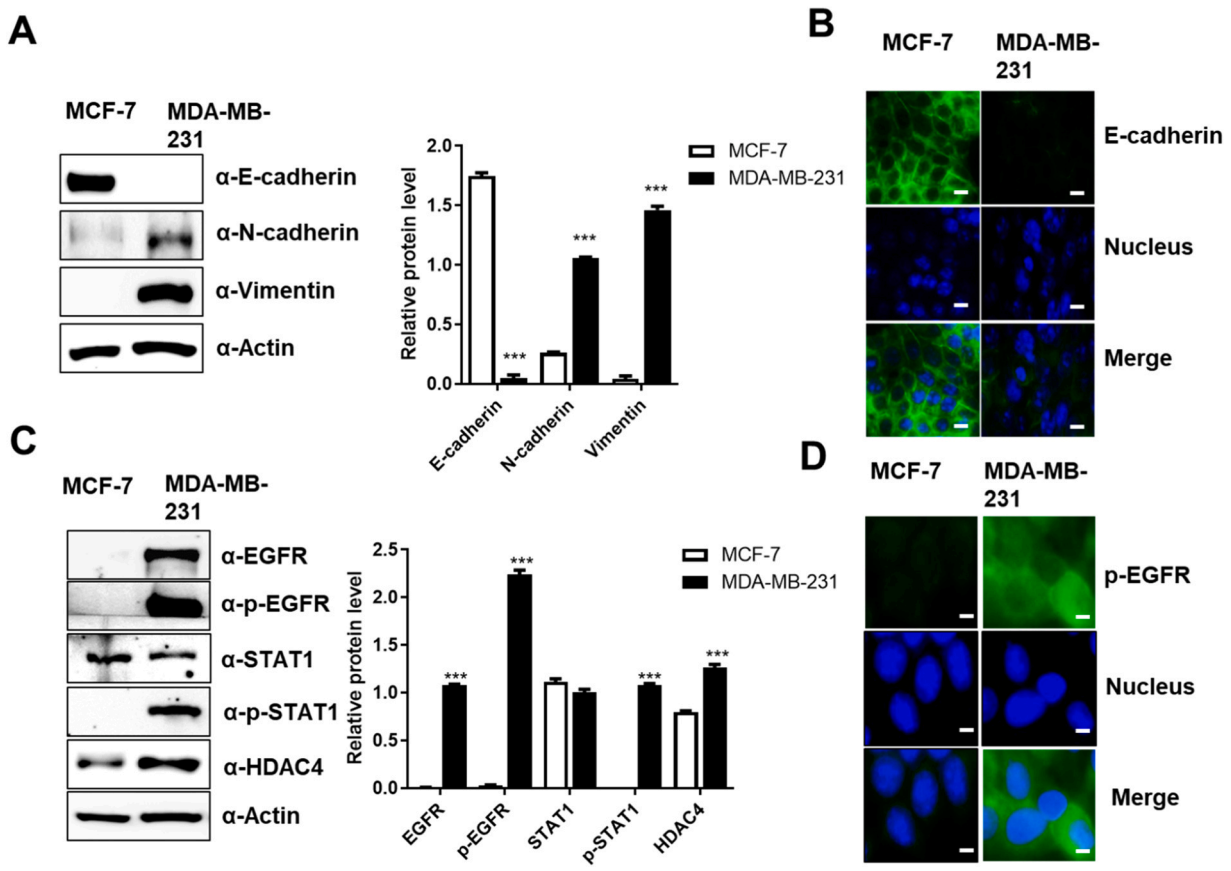

Fig. 1. MDA-MB-231 cells exhibit the elevated expression of EGFR, STAT1 and HDAC4 compared to MCF-7 cells. (A) Cell lysates from MCF-7 and MDA-MB-231 cells were prepared and separated by 10 % SDS-PAGE. The expression of E-cadherin, N-cadherin and vimentin was detected via immunoblotting (compared between MCF-7 and MDA-MB-231 cell lines, $^{***}P < 0.001$). (B) The expression of E-cadherin was detected by immunofluorescence using an Alexa Fluor 488-conjugated secondary antibody (green). DAPI was added for nuclear staining (blue). Scale bar indicates 10 μm. (C) Cell lysates from MCF-7 and MDA-MB-231 cells were prepared and separated by 10 % SDS-PAGE. The expression of EGFR, p-EGFR, STAT1, p-STAT1 and HDAC4 was detected by immunoblotting. (compared between MCF-7 and MDA-MB-231 cell lines, $^{***}P < 0.001$). (D) The expression of p-EGFR was detected by immunofluorescence using an Alexa Fluor 488-conjugated secondary antibody (green). DAPI was added for nuclear staining (blue). Scale bar indicates 50 μm.

or HDAC4 in metastatic MDA-MB 231 breast cancer cells compared to those in nonmetastatic MCF-7 breast cancer cells (Fig. 1), we next investigated whether these proteins are closely associated with EMT progression in the MDA-MB 231 cells. To test our hypothesis, siRNAs against EGFR, STAT1 and HDAC4 were introduced in MDA-MB 231 cells. Silencing EGFR, STAT1 or HDAC4 reduced wound healing of the scratch made in the MDA-MB-231 cells (Fig. 2A). Silencing EGFR, STAT1 or HDAC4 also inhibited cell invasion (Fig. 2B). Supporting these results, the knockdown of EGFR, STAT1 or HDAC4 increased the E-cadherin levels and decreased N-cadherin and vimentin levels (Fig. 2C). Collectively, these results suggest that EGFR, STAT1 and HDAC4 protein are involved in EMT progression in MDA-MB-231 cells. Previous studies have reported that EGFR, STAT1, and HDAC4 activation is associated with chemoresistance [26–29] and malignant phenotypes such as EMT [25,30]. These studies support our finding that the suppression of EGFR, STAT1 and HDAC4 can inhibit malignant phenotypes, including migration, invasion, and adhesion in MDA-MB-231 cells. Our study demonstrated that the decrease in EGFR, STAT1 and HDAC4 levels by ADGL treatment diminished the expression of mesenchymal protein markers such as N-cadherin and vimentin but enhanced the expression of the epithelial protein marker E-cadherin.

3.3. ADGL inhibits EMT progression in MDA-MB-231 cancer cells

To inhibit the EMT progression of metastatic MDA-MB-231 cells, we isolated ADGL from *A. paniculata* and confirmed its structure by 1 H NMR. After treating the MDA-MB 231 breast cancer cells with ADGL, cell scratch assay was performed. Furthermore, we found that wound healing was decreased in an ADGL dose-dependent manner (Fig. 3A). Cell migration was also reduced upon ADGL treatment in a dose-dependent manner (Fig. 3B). ADGL treatment increased the E-cadherin expression and decreased the expression of N-cadherin and vimentin (Fig. 3C). These results suggest that ADGL inhibits EMT progression in MDA-MB-231 breast cancer cells. Some other natural compounds have also been shown to target EGFR, thereby inhibiting EMT [29,31,32]. For example, propolin C, a c-prenylflavanone from Taiwanese propolis, decreased EGF-mediated EMT by inhibiting the Akt-ERK signaling axis [29]. Honokiol, purified from the bark of traditional Chinese herbal Magnolia species exerted inhibitory action on the EGFR-Akt-STAT3 signaling pathway, leading to EMT [31]. Curcumin, a natural polyphenol compound derived from turmeric, also exhibited anti-inhibitory effect on EMT by targeting EGFR signaling [32].

3.4. ADGL suppresses the expression and activity of EGFR, STAT1, and HDAC4 in MDA-MB-231 breast cancer cells

As we observed that ADGL treatment inhibited EMT progression in MDA-MB-231 breast cancer cells (Fig. 3), we investigated whether ADGL treatment diminishes the expression and activities of EGFR, STAT1 and HDAC4, thus impeding EMT progression. We examined the expressions and activities of EGFR, STAT1 and HDAC4. We found that ADGL treatment did not reduce the expression levels of EGFR even at 10 μg/mL;

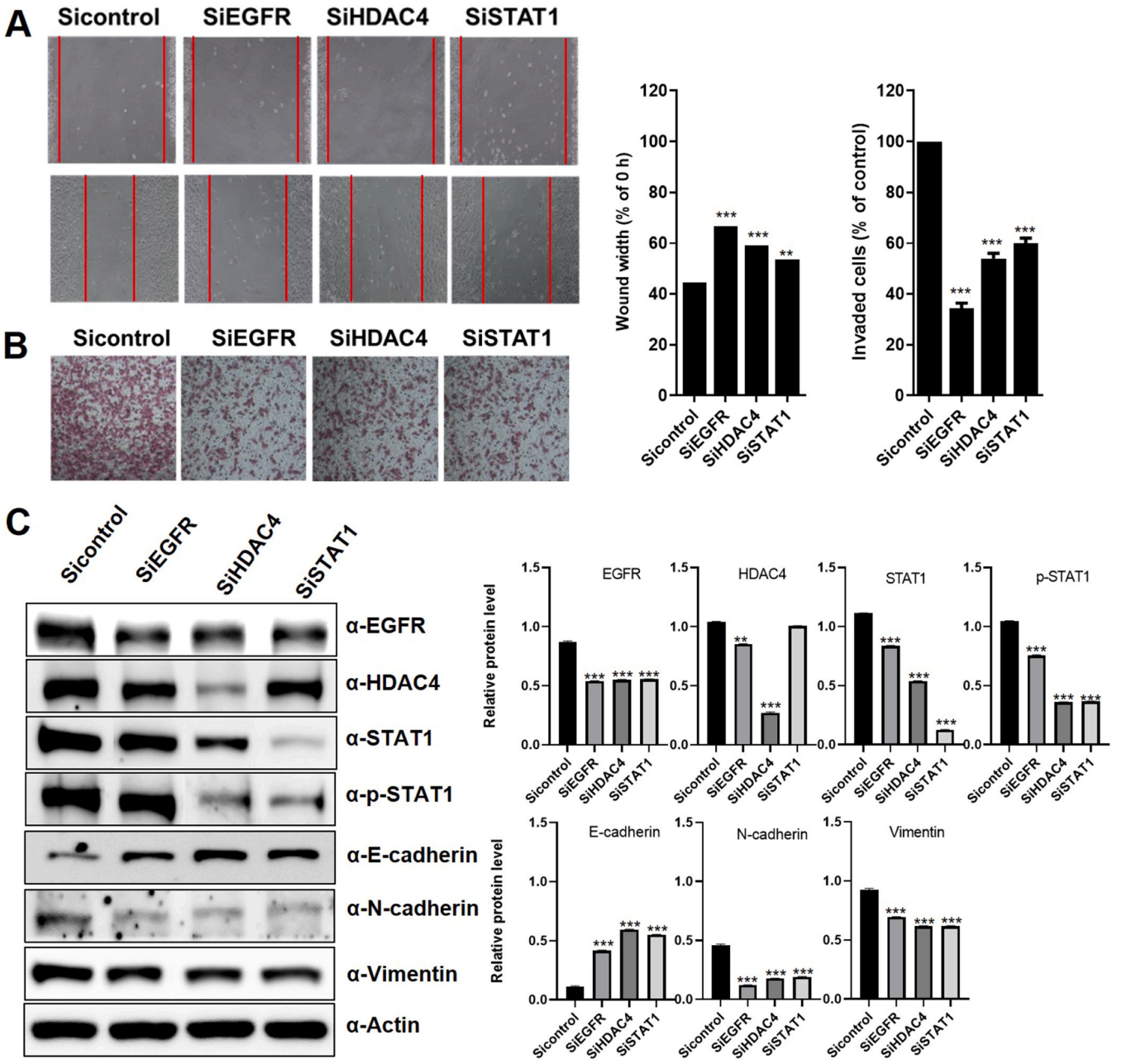

Fig. 2. Silencing of EGFR, STAT1 or HDAC4 inhibits EMT in MDA-MB-231 breast cancer cells. (A) MDA-MB-231 cell migration was measured by a wound healing assay at 24 h post-transfection with SiRNAs against EGFR, HDAC4 or STAT1 (100 nM) and Sicontrol (compared between SiEGFR, SiHDAC4 and SiSTAT1, ***P <0.001). (B) An invasion assay was performed using 48-well Boyden chambers coated with Matrigel at 24 h post-transfection with siRNAs against EGFR, HDAC4 or STAT1 and control siRNA (compared between SiEGFR, SiHDAC4 and SiSTAT1, ***P< 0.001). (C) To examine the effect of EGFR, HDAC4 and STAT1 on the protein levels related to EMT signaling, the expression of EGFR, HDAC4, STAT1, p-STAT1, E-cadherin, N-cadherin and vimentin was detected by immunoblotting at 24 h posttreatment with SiRNAs against EGFR, HDAC4 or STAT1 and control SiRNA (compared between each proteins level of Sicontrol and SiEGFR, SiHDAC4 and SiSTAT1-siRNA, **P< 0.01, ***P< 0.001).

however, it inhibited the phosphorylation of EGFR at 1 μg/mL, indicating that ADGL inhibits EGFR kinase activity at 1 μg/mL concentration (Fig. 4A). Immunofluorescence also confirmed that the ADGL treatment decreased the fluorescent staining of phospho-EGFR intensity which was mainly found in the nucleus (Fig. 4B) as other studies showed phospho-EGFR was detected in the nucleus [33,34]. ADGL treatment did not decrease the STAT1 expression; however, it diminished the phosphorylation levels of STAT1 at 5 μg/mL concentration. HDAC4 expression was also decreased at 5 μg/mL of ADGL (Fig. 4A). Furthermore, when we treated ADGL under suppression of EGFR, STAT1 or HDAC4, we found that cotreatment with ADGL plus EGFR siRNA, ADGL plus STAT1 siRNA or ADGL plus HDAC4 siRNA highly sensitizes MDA-MB-231 cells to apoptosis rather than cotreatment with ADGL plus control siRNA (Fig. 4C). These results suggest that ADGL targets the EGFR-STAT1-HDAC4 signaling axis, resulting in sensitization of apoptosis in MDA-MB-231 cells.

4. Conclusion

In conclusion, we report the role of the EGFR-STAT1-HDAC4 signaling axis in the upregulation of cell motility in addition to their antiapoptotic function in human breast cancer cells. Moreover, ADGL as

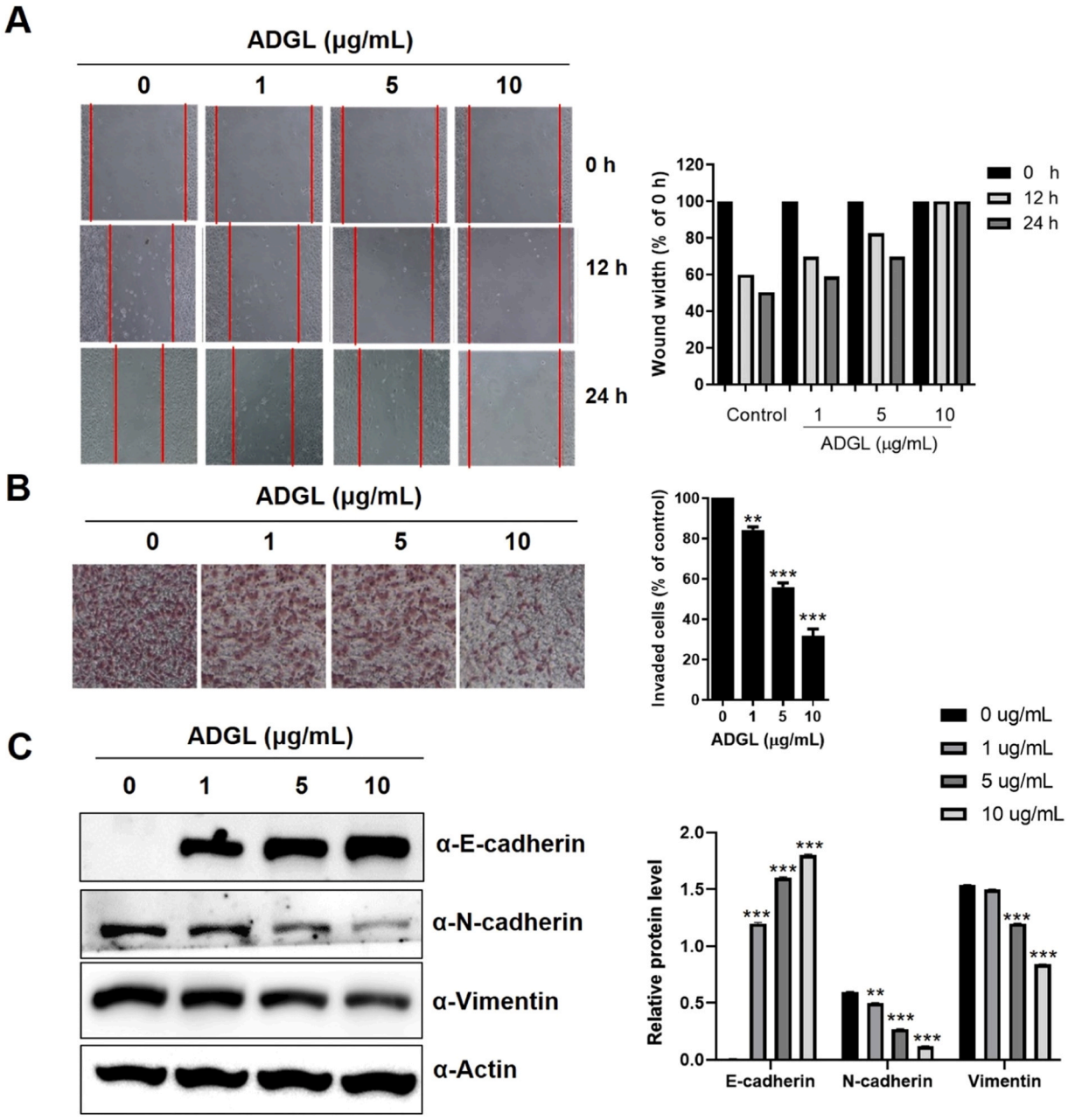

Fig. 3. ADGL inhibits EMT progression in MDA-MB-231 cancer cells. (A) MDA-MB-231 cell migration was measured by a wound healing assay at 12 and 24 h post-treatment with ADGL (***$P < 0.001$ and **$P < 0.01$). (B) An invasion assay was performed using 48-well Boyden chambers coated with Matrigel at 24 and 48 h post-treatment of MDA-MB-231 cells with ADGL. (***$P < 0.001$ and **$P < 0.01$). (C) Cell lysates from MDA-MB-231 cells in the presence or absence of ADGL after 12 h were prepared and separated by 12 % SDS-PAGE. The expression of E-cadherin, N-cadherin and vimentin protein was detected by immunoblotting with the corresponding antibodies (compared between each proteins levels of control and ADGL treated at 1, 5 and 10 ug/mL, **$P< 0.01$, ***$P< 0.001$).

a natural compound can suppress breast cancer cell proliferation, metastasis and invasion by inhibiting the EGFR-STAT1-HDAC4 signaling pathway.

Ethical considerations

This study does not involve the use of animal or human models. Ethical issues (including plagiarism, misconduct, data fabrication, falsification, double publication or submission, redundancy) have been ultimately observed by the authors.

CRediT authorship contribution statement

Abdulwahab Salae: Data curation, Formal analysis. **Chutima Kaewpiboon:** Writing – review & editing, Writing – original draft, Validation, Methodology, Investigation, Conceptualization. **Nawong Boonnak:** Validation. **Young-Hwa Chung:** Writing – review & editing, Project administration, Funding acquisition, Conceptualization. **Sirichatnach Pakdeepromma:** Formal analysis. **Natpaphan Yawut:** Investigation.

Declaration of Competing Interest

The authors declare that they have no known competing financial

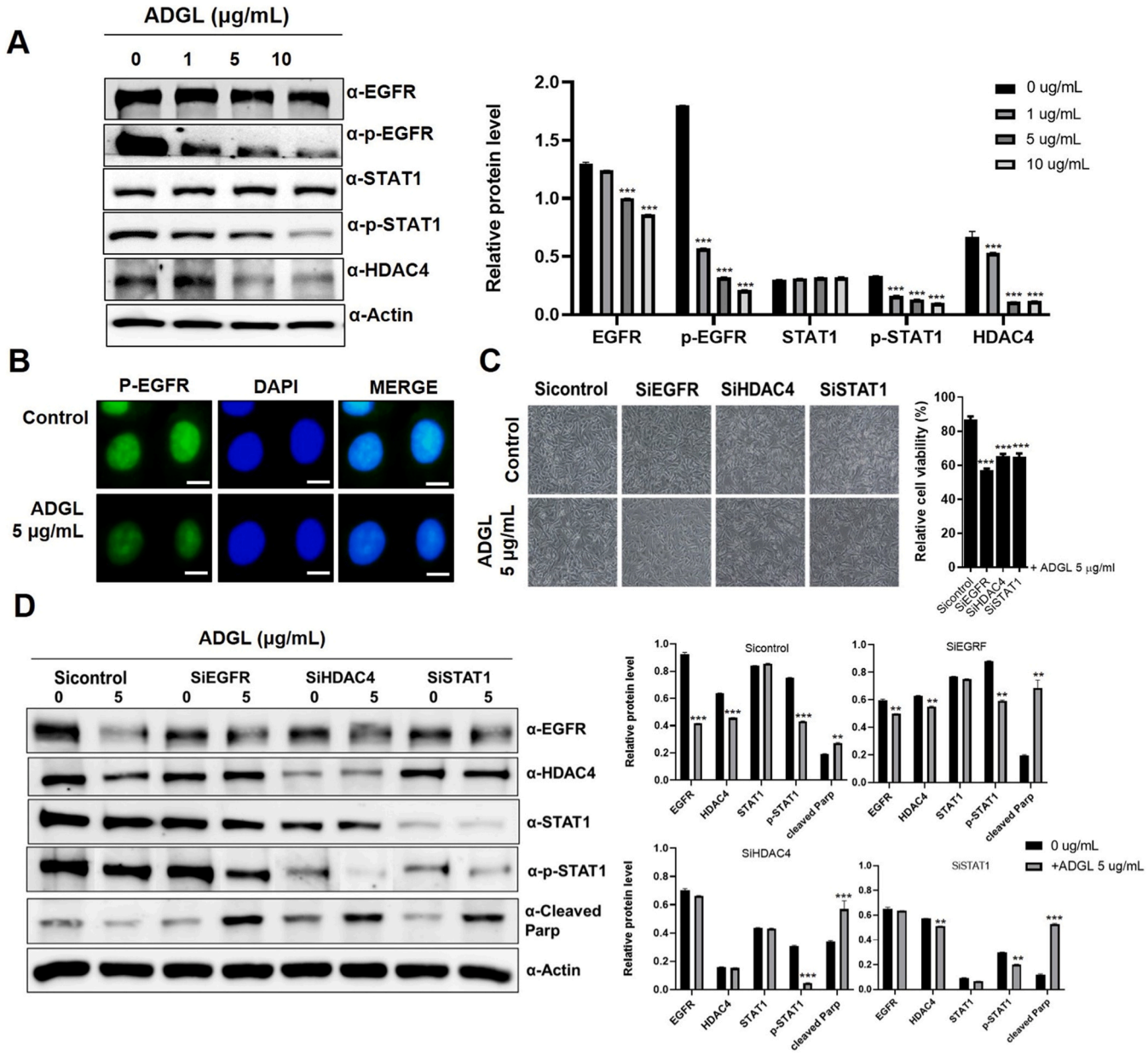

Fig. 4. ADGL suppresses the expression and activity of EGFR, STAT1 and HDAC4 in MDA-MB-231 breast cancer cells. (A) Cell lysates from MDA-MB-231 cells in the presence or absence of ADGL after 12 h were prepared and separated by 10 % SDS-PAGE. The expression of EGFR, p-EGFR, STAT1, p-STAT1, HDAC4, cadherin and vimentin proteins was detected by immunoblotting with the corresponding antibodies. (B) After treatment with ADGL (5.0 μg/mL) for 12 h, phospho-EGFR levels were examined by immunofluorescence using an Alexa Fluor 488-conjugated secondary antibody (green). DAPI was added for nuclear staining (blue). Scale bar indicates 50 μm. (C) MDA-MB-231 cells were treated with ADGL (5.0 μg/mL) for 24 h after transfection with a control siRNA or siRNAs against EGFR, STAT1 or HDAC4 (100 nM). Cell viability was observed under an optical microscope and measured using the MTT assay. The data were calculated as the percentage of relative cell viability and are expressed as the mean of three experiments (control siRNA + ADGL vs. EGFR-, STAT1- and HDAC4- siRNA + ADGL; $^{***}P< 0.001$). (D) Cell lysates from the treated MDA-MB-231 cells were prepared and separated by 12 % SDS-PAGE. The expression of EGFR, HDAC4, STAT1, p-STAT1 and cleaved PARP proteins was detected by immunoblotting with the corresponding antibodies (compared between each proteins levels of control and ADGL treated at 0 and 5μg/mL, $^{**}P< 0.01$, $^{***}P< 0.001$).

interests or personal relationships that could have appeared to influence the work reported in this paper.

Acknowledgments

We sincerely thank the Korea Institute for Advancement of Technology (KIAT) in Republic of Korea for financial support (Grant No. N0002310, Construction Project of Supporting Center for Commercializing Customized Nano-mold-based Technologies).

Appendix A. Supporting information

Supplementary data associated with this article can be found in the online version at doi:10.1016/j.jpba.2024.116267.

References

[1] L.T.H. Phi, I.N. Sari, Y.-G. Yang, S.-H. Lee, N. Jun, K.S. Kim, Y.K. Lee, H.Y. Kwon, Cancer stem cells (CSCs) in drug resistance and their therapeutic implications in cancer treatment, Stem Cells Int. 2018 (2018) 16.

[2] M.S. Hossain, Z. Urbi, A. Sule, K.M.H. Rahman, Andrographis paniculata (Burm. f.) Wall. ex Nees: a review of ethnobotany, Phytochem., Pharmacol., Sci. World J. 2014 (2014) 28.
[3] Z.G. Chen, R.X. Tan, L. Cao, Efficient and highly regioselective acylation of andrographolide catalyzed by lipase in acetone, Green Chem. 11 (11) (2009) 1743–1745.
[4] P. Panraksa, S. Ramphan, S. Khongwichit, D.R. Smith, Activity of andrographolide against dengue virus, Antivir. Res. 139 (2017) 69–78.
[5] L.G. Vaishali, J.H. Patel, R.D. Varia, S.K. Bhavsar, P.D. Vihol, F. D. Modi, Pharmacokinetics and anti-inflammatory activity of andrographolide in rats, Int. J. Curr. Microbiol. Appl. Sci. 6 (8) (2017) 1458–1463.
[6] M.M. Uttekar, T. Das, R.S. Pawar, B. Bhandari, V. Menon, Nutan, S.K. Gupta, S. V. Bhat, Anti-HIV activity of semisynthetic derivatives of andrographolide and computational study of HIV-1 gp120 protein binding, Eur. J. Med. Chem. 56 (2012) 368–374.
[7] W. Wang, J. Wang, S.F. Dong, C.H. Liu, P. Italiani, S.H. Sun, J. Xu, D. Boraschi, S. P. Ma, D. Qu, Immunomodulatory activity of andrographolide on macrophage activation and specific antibody response, Acta Pharmacol. Sin. 31 (2) (2010) 191–201.
[8] S. Reabroi, R. Saeeng, N. Boonmuen, T. Kasemsuk, W. Saengsawang, K. Suksen, W. Zhu, P. Piyachaturawat, A. Chairoungdua, The anti-cancer activity of an andrographolide analogue functions through a GSK-3beta-independent Wnt/beta-catenin signaling pathway in colorectal cancer cells, Sci. Rep. 8 (1) (2018) 7924.
[9] Y. Peng, Y. Wang, N. Tang, D. Sun, Y. Lan, Z. Yu, X. Zhao, L. Feng, B. Zhang, L. Jin, F. Yu, X. Ma, C. Lv, Andrographolide inhibits breast cancer through suppressing COX-2 expression and angiogenesis via inactivation of p300 signaling and VEGF pathway, J. Exp. Clin. Cancer Res. 37 (1) (2018) 248.
[10] C.-C. Yu, C.-A. Chen, S.-L. Fu, H.-Y. Lin, M.-S. Lee, W.-Y. Chiou, Y.-C. Su, S.-K. Hung, Andrographolide enhances the anti-metastatic effect of radiation in Ras-transformed cells via suppression of ERK–mediated MMP-2 activity, PLOS One 13 (10) (2018) e0205666.
[11] B. Wu, X. Chen, Y. Zhou, P. Hu, D. Wu, G. Zheng, Y. Cai, Andrographolide inhibits proliferation and induces apoptosis of nasopharyngeal carcinoma cell line C666-1 through LKB1-AMPK-dependent signaling pathways, Die Pharm. 73 (10) (2018) 594–597.
[12] C.-Y. Chao, C.-K. Lii, Y.-T. Hsu, C.-Y. Lu, K.-L. Liu, C.-C. Li, H.-W. Chen, Induction of heme oxygenase-1 and inhibition of TPA-induced matrix metalloproteinase-9 expression by andrographolide in MCF-7 human breast cancer cells, Carcinogenesis 34 (8) (2013) 1843–1851.
[13] F. Kayastha, H. Madhu, A. Vasavada, K. Johar, Andrographolide reduces proliferation and migration of lens epithelial cells by modulating PI3K/Akt pathway, Exp. Eye Res. 128 (2014) 23–26.
[14] G.-F. Li, Y.-H. Qin, P.-Q. Du, Andrographolide inhibits the migration, invasion and matrix metalloproteinase expression of rheumatoid arthritis fibroblast-like synoviocytes via inhibition of HIF-1α signaling, Life Sci. 136 (2015) 67–72.
[15] G. Bethune, D. Bethune, N. Ridgway, Z. Xu, Epidermal growth factor receptor (EGFR) in lung cancer: an overview and update, J. Thorac. Dis. 2 (1) (2010) 48–51.
[16] M. Westphal, C.L. Maire, K. Lamszus, EGFR as a target for glioblastoma treatment: an unfulfilled promise, CNS Drugs 31 (9) (2017) 723–735.
[17] J.A. Wilken, T. Badri, S. Cross, R. Raji, A.D. Santin, P. Schwartz, A.J. Branscum, A. T. Baron, A.I. Sakhitab, N.J. Maihle, EGFR/HER-targeted therapeutics in ovarian cancer, Future Med. Chem. 4 (4) (2012) 447–469.
[18] H. Masuda, D. Zhang, C. Bartholomeusz, H. Doihara, G.N. Hortobagyi, N.T. Ueno, Role of epidermal growth factor receptor in breast cancer, Breast Cancer Res. Treat. 136 (2) (2012) 331–345.
[19] S. Sigismund, D. Avanzato, L. Lanzetti, Emerging functions of the EGFR in cancer, Mol. Oncol. 12 (1) (2018) 3–20.
[20] S. Chantrapromma, N. Boonnak, T. Pitakpornpreecha, T. Yordthong, C.S. Chidan Kumar, H.K. Fun, Absolute configuration of andrographolide and its proliferation of osteoblast cell lines, Crystallogr. Rep. 63 (3) (2018) 412–417.
[21] C. Kaewpiboon, K. Lirdprapamongkol, C. Srisomsap, P. Winayanuwattikun, T. Yongvanich, P. Puwaprisirisan, J. Svasti, W. Assavalapsakul, Studies of the in vitro cytotoxic, antioxidant, lipase inhibitory and antimicrobial activities of selected Thai medicinal plants, BMC Complement Alter. Med. 12 (2012) 217.
[22] B. Dave, V. Mittal, N.M. Tan, J.C. Chang, Epithelial-mesenchymal transition, cancer stem cells and treatment resistance, Breast Cancer Res. 14 (1) (2012) 202.
[23] Y. Tsubakihara, A. Moustakas, Epithelial-mesenchymal transition and metastasis under the control of transforming growth factor beta, Int. J. Mol. Sci. 19 (11) (2018).
[24] T. Yoshimura, T. Hamada, H. Hijioka, M. Souda, K. Hatanaka, T. Yoshioka, S. Yamada, M. Tsutsui, Y. Umekita, N. Nakamura, A. Tanimoto, PCP4/PEP19 promotes migration, invasion and adhesion in human breast cancer MCF-7 and T47D cells, Oncotarget 7 (31) (2016) 49065–49074.
[25] S. Kaowinn, C. Kaewpiboon, S.S. Koh, O.H. Krämer, Y.-H. Chung, STAT1-HDAC4 signaling induces epithelial-mesenchymal transition and sphere formation of cancer cells overexpressing the oncogene, CUG2, Oncol. Rep. 40 (5) (2018) 2619–2627.
[26] E.A. Stronach, A. Alfraidi, N. Rama, C. Datler, J.B. Studd, R. Agarwal, T.G. Guney, C. Gourley, B.T. Hennessy, G.B. Mills, A. Mai, R. Brown, R. Dina, H. Gabra, HDAC4-regulated STAT1 activation mediates platinum resistance in ovarian cancer, Cancer Res. 71 (13) (2011) 4412–4422.
[27] C. Kaewpiboon, R. Srisuttee, W. Malilas, J. Moon, S. Oh, H.G. Jeong, R. N. Johnston, W. Assavalapsakul, Y.H. Chung, Upregulation of Stat1-HDAC4 confers resistance to etoposide through enhanced multidrug resistance 1 expression in human A549 lung cancer cells, Mol. Med. Rep. 11 (3) (2015) 2315–2321.
[28] S. Kaowinn, S.W. Jun, C.S. Kim, D.M. Shin, Y.H. Hwang, K. Kim, B. Shin, C. Kaewpiboon, H.H. Jeong, S.S. Koh, O.H. Kramer, R.N. Johnston, Y.H. Chung, Increased EGFR expression induced by a novel oncogene, CUG2, confers resistance to doxorubicin through Stat1-HDAC4 signaling, Cell Oncol. 40 (6) (2017) 549–561.
[29] J.-T. Pai, Y.-C. Lee, S.-Y. Chen, Y.-L. Leu, M.-S. Weng, Propolin C inhibited migration and invasion via suppression of EGFR-mediated epithelial-to-mesenchymal transition in human lung cancer cells, evidence-based complementary and alternative medicine, eCAM 2018 (2018), 7202548-7202548.
[30] N. Normanno, A. De Luca, C. Bianco, L. Strizzi, M. Mancino, M.R. Maiello, A. Carotenuto, G. De Feo, F. Caponigro, D.S. Salomon, Epidermal growth factor receptor (EGFR) signaling in cancer, Gene 366 (1) (2006) 2–16.
[31] J. Pan, Y. Lee, Q. Zhang, D. Xiong, T.C. Wan, Y. Wang, M. You, Honokiol decreases lung cancer metastasis through inhibition of the STAT3 signaling pathway, Cancer Prev. Res. 10 (2) (2017) 133–141.
[32] W. Li, Z. Jiang, X. Xiao, Z. Wang, Z. Wu, Q. Ma, L. Cao, Curcumin inhibits superoxide dismutase-induced epithelial-to-mesenchymal transition via the PI3K/Akt/NF-κB pathway in pancreatic cancer cells, Int. J. Oncol. 52 (2018) 1593–1602.
[33] M. Hoshino, H. Fukui, Y. Ono, A. Sekikawa, K. Ichikawa, S. Tomita, Y. Imai, J. Imura, H. Hiraishi, T. Fujimori, Nuclear expression of phosphorylated EGFR is associated with poor prognosis of patients with esophageal squamous cell carcinoma, Pathobiol.: J. Immunopathol., Mol. Cell. Biol. 74 (1) (2007) 15–21.
[34] C.C. Yang, L.C. Lin, Y.W. Lin, Y.F. Tian, C.Y. Lin, M.J. Sheu, C.F. Li, M.H. Tai, Higher nuclear EGFR expression is a better predictor of survival in rectal cancer patients following neoadjuvant chemoradiotherapy than cytoplasmic EGFR expression, Oncol. Lett. 17 (2) (2019) 1551–1558.